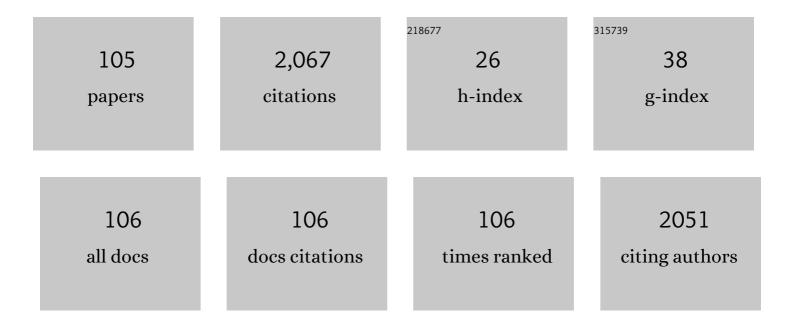
Sunando DasGupta

List of Publications by Year in descending order

Source: https://exaly.com/author-pdf/5442031/publications.pdf Version: 2024-02-01



#	Article	lF	CITATIONS
1	Molecular Investigation of the Actuation of Electrowetted Nanodroplets. Langmuir, 2022, 38, 3656-3665.	3.5	4
2	Mechanistic Underpinnings of Morphology Transition in Electrodeposition under the Application of Pulsatile Potential. Langmuir, 2022, , .	3.5	5
3	Electro-osmosis Aided Thin-Film Evaporation from a Micropillar Wick Structure. Langmuir, 2022, 38, 8442-8455.	3.5	2
4	Evaporation mediated translation and encapsulation of an aqueous droplet atop a viscoelastic liquid film. Journal of Colloid and Interface Science, 2021, 581, 334-349.	9.4	7
5	Development of graphene oxide – PDMS composite dielectric for rapid droplet movement in digital microfluidic applications. Chemical Engineering Science, 2021, 230, 116175.	3.8	8
6	Role of anisotropic pinning and liquid properties during partial rebound of droplets on unidirectionally structured hydrophobic surfaces. Chemical Engineering Science, 2021, 230, 116197.	3.8	8
7	Analysis of augmented droplet transport during electrowetting over triangular coplanar electrode array. Journal of Electrostatics, 2021, 109, 103541.	1.9	8
8	Performance evaluation of evaporation from micropillar arrays with different pillar topologies. International Journal of Thermal Sciences, 2021, 168, 107044.	4.9	5
9	Rapid determination of erythrocyte sedimentation rate (ESR) by an electrically driven blood droplet biosensor. Biomicrofluidics, 2020, 14, 064108.	2.4	4
10	Temperature-gradient-induced massive augmentation of solute dispersion in viscoelasticÂmicro-flows. Journal of Fluid Mechanics, 2020, 897, .	3.4	6
11	Interfacial energy driven distinctive pattern formation during the drying of blood droplets. Journal of Colloid and Interface Science, 2020, 573, 307-316.	9.4	13
12	Nano-particles in optimal concentration facilitate electrically driven dynamic spreading of a drop on a soft viscoelastic solid. Physics of Fluids, 2020, 32, .	4.0	8
13	Biomimetic pulsatile flows through flexible microfluidic conduits. Biomicrofluidics, 2019, 13, 014103.	2.4	11
14	Patterned surface charges coupled with thermal gradients may create giant augmentations of solute dispersion in electro-osmosis of viscoelastic fluids. Proceedings of the Royal Society A: Mathematical, Physical and Engineering Sciences, 2019, 475, 20180522.	2.1	9
15	Electrowetting of a nano-suspension on a soft solid. Applied Physics Letters, 2019, 114, .	3.3	13
16	Tunable adhesion and slip on a bio-mimetic sticky soft surface. Soft Matter, 2019, 15, 9031-9040.	2.7	13
17	Replicating and resolving wetting and adhesion characteristics of a Rose petal. Colloids and Surfaces A: Physicochemical and Engineering Aspects, 2019, 561, 9-17.	4.7	71
18	Field-Assisted Contact Line Motion in Thin Films. Langmuir, 2018, 34, 12665-12679.	3.5	0

#	Article	IF	CITATIONS
19	Droplets in Microfluidics. Energy, Environment, and Sustainability, 2018, , 347-379.	1.0	1
20	Rapid estimation of the β-sheet content of Human Serum Albumin from the drying patterns of HSA-nanoparticle droplets. Colloids and Surfaces A: Physicochemical and Engineering Aspects, 2018, 540, 177-185.	4.7	8
21	Anisotropic Electrowetting on Wrinkled Surfaces: Enhanced Wetting and Dependency on Initial Wetting State. Langmuir, 2018, 34, 1844-1854.	3.5	16
22	Collective dynamics of red blood cells on an <i>in vitro</i> microfluidic platform. Lab on A Chip, 2018, 18, 3939-3948.	6.0	17
23	Analysis of the Distinct Pattern Formation of Clobular Proteins in the Presence of Micro- and Nanoparticles. Journal of Physical Chemistry B, 2018, 122, 8972-8984.	2.6	16
24	Fractal Dimension of Erythrocyte Membranes: A Highly Useful Precursor for Rapid Morphological Assay. Annals of Biomedical Engineering, 2018, 46, 1362-1375.	2.5	2
25	Flow-induced deformation in a microchannel with a non-Newtonian fluid. Biomicrofluidics, 2018, 12, 034116.	2.4	28
26	Tailored topography: a novel fabrication technique using an elasticity gradient. Soft Matter, 2018, 14, 7034-7044.	2.7	10
27	Electrodewetting and Wetting of an Extended Meniscus. Langmuir, 2018, 34, 9897-9906.	3.5	3
28	Surface property induced morphological alterations of human erythrocytes. Soft Matter, 2018, 14, 7335-7346.	2.7	9
29	Oscillating nanofluid droplet for micro-cooling. Sensors and Actuators B: Chemical, 2017, 239, 562-570.	7.8	18
30	Fibrillar disruption by AC electric field induced oscillation: A case study with human serum albumin. Biophysical Chemistry, 2017, 226, 23-33.	2.8	8
31	Capillary driven flow in wettability altered microchannel. AICHE Journal, 2017, 63, 4616-4627.	3.6	4
32	Inhibition of Human Serum Albumin Fibrillation by Two-Dimensional Nanoparticles. Journal of Physical Chemistry B, 2017, 121, 5474-5482.	2.6	34
33	Hydrodynamics in deformable microchannels. Microfluidics and Nanofluidics, 2017, 21, 1.	2.2	38
34	Magnetowetting of Ferrofluidic Thin Liquid Films. Scientific Reports, 2017, 7, 44738.	3.3	13
35	Electroosmosis of Viscoelastic Fluids: Role of Wall Depletion Layer. Langmuir, 2017, 33, 12046-12055.	3.5	35
36	Does Surface Chirality of Gold Nanoparticles Affect Fibrillation of HSA?. Journal of Physical Chemistry C, 2017, 121, 18935-18946.	3.1	26

#	Article	IF	CITATIONS
37	Ion-size dependent electroosmosis of viscoelastic fluids in microfluidic channels with interfacial slip. Physics of Fluids, 2017, 29, 072002.	4.0	25
38	Inhibition of fibrillation of human serum albumin through interaction with chitosan-based biocompatible silver nanoparticles. RSC Advances, 2016, 6, 43104-43115.	3.6	32
39	Hydropathy: the controlling factor behind the inhibition of AÎ ² fibrillation by graphene oxide. RSC Advances, 2016, 6, 103242-103252.	3.6	12
40	Contact Line Dynamics during the Evaporation of Extended Colloidal Thin Films: Influence of Liquid Polarity and Particle Size. Langmuir, 2016, 32, 12790-12798.	3.5	3
41	Hydrophobic tail length plays a pivotal role in amyloid beta (25-35) fibril-surfactant interactions. Proteins: Structure, Function and Bioinformatics, 2016, 84, 1213-1223.	2.6	20
42	Thermally enhanced self-propelled droplet motion on gradient surfaces. RSC Advances, 2015, 5, 45266-45275.	3.6	30
43	Effect of Surface Wettability on Crack Dynamics and Morphology of Colloidal Films. Langmuir, 2015, 31, 6001-6010.	3.5	25
44	Interfacial force-driven pattern formation during drying of Aβ (25–35) fibrils. International Journal of Biological Macromolecules, 2015, 79, 344-352.	7.5	8
45	Experimental and Theoretical Evaluation of On-Chip Micro Heat Pipe. Nanoscale and Microscale Thermophysical Engineering, 2015, 19, 75-93.	2.6	8
46	Effect of air sparging on flux enhancement during tangential flow filtration of degreasing effluent. Desalination and Water Treatment, 2015, 53, 73-83.	1.0	2
47	Electrowetting of Partially Wetting Thin Nanofluid Films. Langmuir, 2015, 31, 4160-4168.	3.5	17
48	Dynamics of Electrically Modulated Colloidal Droplet Transport. Langmuir, 2015, 31, 11269-11278.	3.5	19
49	Taylor–Aris dispersion induced by axial variation in velocity profile in patterned microchannels. Chemical Engineering Science, 2015, 134, 251-259.	3.8	10
50	Molecular Dynamics Study of Thermally Augmented Nanodroplet Motion on Chemical Energy Induced Wettability Gradient Surfaces. Langmuir, 2015, 31, 11260-11268.	3.5	31
51	Enhanced microcooling by electrically induced droplet oscillation. RSC Advances, 2014, 4, 1074-1082.	3.6	19
52	Effect of Functionalized Magnetic MnFe ₂ O ₄ Nanoparticles on Fibrillation of Human Serum Albumin. Journal of Physical Chemistry B, 2014, 118, 11667-11676.	2.6	45
53	Disruption of human serum albumin fibrils by a static electric field. Journal Physics D: Applied Physics, 2014, 47, 305401.	2.8	17
54	Membrane Applications in Fruit Processing Technologies. Contemporary Food Engineering, 2012, , 87-148.	0.2	2

4

#	Article	IF	CITATIONS
55	Electrowetting of evaporating extended meniscus. Soft Matter, 2012, 8, 11302.	2.7	8
56	Electric Field Enhanced Spreading of Partially Wetting Thin Liquid Films. Langmuir, 2011, 27, 12951-12959.	3.5	15
57	Effect of submicron particles on electrowetting on dielectrics (EWOD) of sessile droplets. Journal of Colloid and Interface Science, 2011, 363, 640-645.	9.4	26
58	Experimental investigation of enhanced spreading and cooling from a microgrooved surface. Microfluidics and Nanofluidics, 2011, 11, 489-499.	2.2	12
59	Treatment of dyeing effluent from tannery using membrane separation processes. International Journal of Environment and Waste Management, 2010, 5, 354.	0.3	9
60	Quantification of transient flux decline during membrane separation of tanning effluent from tannery. International Journal of Environmental Engineering, 2010, 2, 31.	0.1	0
61	Microscale Transport Processes and Interfacial Force Field Characterization in Micro-cooling Devices. , 2010, , 113-130.		0
62	PERFORMANCE PREDICTION OF MEMBRANE MODULES INCORPORATING THE EFFECTS OF SUCTION IN THE MASS TRANSFER COEFFICIENT UNDER LAMINAR AND TURBULENT FLOW CONDITIONS FOR NONâ€NEWTONIAN FLUIDS. Journal of Food Process Engineering, 2009, 32, 752-774.	2.9	1
63	Flux decline during electric field-assisted cross-flow ultrafiltration of mosambi (Citrus sinensis (L.)) Tj ETQq1 1 0.78	84314 rgB 8.2	T ₁ /Overlock
64	Electric field enhanced fractionation of protein mixture using ultrafiltration. Journal of Membrane Science, 2009, 341, 11-20.	8.2	28
65	Prediction of permeate flux during electric field enhanced cross-flow ultrafiltration—A neural network approach. Separation and Purification Technology, 2009, 65, 260-268.	7.9	65
66	Application of external electric field to enhance the permeate flux during micellar enhanced ultrafiltration. Separation and Purification Technology, 2009, 66, 263-272.	7.9	25
67	Flux enhancement by argon–oxygen plasma treatment of polyethersulfone membranes. Separation and Purification Technology, 2009, 70, 160-165.	7.9	58
68	Evaluation of surface roughness of a plasma treated polymeric membrane by wavelet analysis and quantification of its enhanced performance. Applied Surface Science, 2008, 255, 2504-2511.	6.1	42
69	An experimental and theoretical analysis of turbulence promoter assisted ultrafiltration of synthetic fruit juice. Separation and Purification Technology, 2008, 62, 659-667.	7.9	36
70	Steadyâ€state modeling for membrane separation of pretreated soaking effluent under cross flow mode. Environmental Progress, 2008, 27, 346-352.	0.7	4
71	Prediction of permeate flux during osmotic pressure-controlled electric field-enhanced cross-flow ultrafiltration. Journal of Colloid and Interface Science, 2008, 319, 236-246.	9.4	16
72	Effect of electric field during gel-layer controlled ultrafiltration of synthetic and fruit juice. Journal of Membrane Science, 2008, 307, 268-276.	8.2	38

#	Article	IF	CITATIONS
73	Optical evaluation of deposition thickness and measurement of permeate flux enhancement of simulated fruit juice in presence of turbulence promoters. Journal of Membrane Science, 2008, 315, 58-66.	8.2	17
74	Pulsed electric field enhanced ultrafiltration of synthetic and fruit juice. Separation and Purification Technology, 2008, 63, 582-591.	7.9	26
75	Cross-flow electro-ultrafiltration of mosambi (Citrus sinensis (L.) Osbeck) juice. Journal of Food Engineering, 2008, 89, 241-245.	5.2	22
76	A study of electric field enhanced ultrafiltration of synthetic fruit juice and optical quantification of gel deposition. Journal of Membrane Science, 2008, 311, 112-120.	8.2	39
77	Simultaneous Separation of Mixture of Metal Ions and Aromatic Alcohol using Cross Flow Micellarâ€Enhanced Ultrafiltration and Recovery of Surfactant. Separation Science and Technology, 2008, 43, 71-92.	2.5	7
78	Treatment of Liming Effluent from Tannery using Membrane Separation Processes. Separation Science and Technology, 2007, 42, 517-539.	2.5	8
79	Experimental Investigation of Evaporation and Condensation in the Contact Line Region of a Thin Liquid Film Experiencing Small Thermal Perturbations. Langmuir, 2007, 23, 1234-1241.	3.5	17
80	Treatment of soaking effluent from a tannery using membrane separation processes. Desalination, 2007, 216, 160-173.	8.2	20
81	Performance prediction of membrane modules incorporating the effects of suction in the mass transfer coefficient under turbulent flow conditions. Separation and Purification Technology, 2007, 55, 182-190.	7.9	3
82	Adsorption of Reactive Dyes from a Textile Effluent Using Sawdust as the Adsorbent. Industrial & Engineering Chemistry Research, 2006, 45, 4732-4741.	3.7	24
83	Response to "Comment on â€~Adsorption of Reactive Dyes from a Textile Effluent Using Sawdust as the Adsorbent'Â― Industrial & Engineering Chemistry Research, 2006, 45, 7363-7363.	3.7	2
84	Treatment of tanning effluent using nanofiltration followed by reverse osmosis. Separation and Purification Technology, 2006, 50, 291-299.	7.9	81
85	Optical quantification of fouling during nanofiltration of dyes. Separation and Purification Technology, 2006, 52, 372-379.	7.9	15
86	A model of the capillary limit of a micro heat pipe and prediction of the dry-out length. International Journal of Heat and Fluid Flow, 2005, 26, 495-505.	2.4	57
87	Transient modeling of micro-grooved heat pipe. International Journal of Heat and Mass Transfer, 2005, 48, 1633-1646.	4.8	51
88	Performance prediction of turbulent promoter enhanced nanofiltration of a dye solution. Separation and Purification Technology, 2005, 43, 85-94.	7.9	10
89	Performance prediction of membrane modules incorporating the effects of suction in the mass transfer coefficient under laminar flow conditions. Separation and Purification Technology, 2005, 45, 109-118.	7.9	2
90	Experimental Determination of the Effect of Disjoining Pressure on Shear in the Contact Line Region of a Moving Evaporating Thin Film. Journal of Heat Transfer, 2005, 127, 231-243.	2.1	51

#	Article	IF	CITATIONS
91	Reflectivity-based evaluation of the coalescence of two condensing drops and shape evolution of the coalesced drop. Physical Review E, 2004, 70, 051610.	2.1	33
92	Inferred pressure gradient and fluid flow in a condensing sessile droplet based on the measured thickness profile. Physics of Fluids, 2004, 16, 1942-1955.	4.0	51
93	Flux enhancement in nanofiltration of dye solution using turbulent promoters. Separation and Purification Technology, 2004, 40, 31-39.	7.9	29
94	A study of the oscillating corner meniscus in a vertical constrained vapor bubble system. Superlattices and Microstructures, 2004, 35, 559-572.	3.1	15
95	Mass transfer coefficient with suction for laminar non-Newtonian flow in application to membrane separations. Journal of Food Engineering, 2004, 64, 53-61.	5.2	14
96	Mass transfer coefficient with suction for turbulent non-Newtonian flow in application to membrane separations. Journal of Food Engineering, 2004, 65, 533-541.	5.2	7
97	A Study of an Oscillating Corner Meniscus With Phase Change Using Image Analyzing Interferometry. , 2004, , 317.		0
98	Removal of Cresol from Aqueous Solution Using Fly Ash as Adsorbent: Experiments and Modeling. Separation Science and Technology, 2003, 38, 1345-1360.	2.5	18
99	Modeling and simulation of osmotic pressure controlled electro-ultrafiltration in a cross-flow system. Journal of Membrane Science, 2002, 199, 29-40.	8.2	10
100	Modeling of cross-flow osmotic pressure controlled membrane separation processes under turbulent flow conditions. Journal of Membrane Science, 2002, 201, 203-212.	8.2	8
101	Experimental and theoretical study of axial dryout point for evaporation from V-shaped microgrooves. International Journal of Heat and Mass Transfer, 2002, 45, 1535-1543.	4.8	40
102	Prediction of mass transfer coefficient with suction for turbulent flow in cross flow ultrafiltration. Journal of Membrane Science, 1999, 157, 227-239.	8.2	45
103	MODELING OF EVAPORATION FROM V-SHAPED MICROGROOVES. Chemical Engineering Communications, 1997, 160, 225-248.	2.6	15
104	Interfacial force field characterization in a constrained vapor bubble thermosyphon. AICHE Journal, 1995, 41, 2140-2149.	3.6	49
105	Use of the Augmented Young-Laplace Equation to Model Equilibrium and Evaporating Extended Menisci. Journal of Colloid and Interface Science, 1993, 157, 332-342.	9.4	75

7